

# Investigating The Effect of Piezoelectric Material Type on Biomechanical Energy Harvesting Efficiency

Thashayani Sathasivam<sup>1</sup>, Nur Hidayah Mansor<sup>1\*</sup>

<sup>1</sup> School of Mechanical Engineering, Engineering Campus,  
Universiti Sains Malaysia, 14300, Nibong Tebal, Pulau Pinang, MALAYSIA

\*Corresponding Author: [menurhidayah@usm.my](mailto:menurhidayah@usm.my)  
DOI: <https://doi.org/10.30880/ijie.2025.17.08.004>

## Article Info

Received: 1 June 2025

Accepted: 20 November 2025

Available online: 31 December 2025

## Keywords

Piezoelectric energy harvesters,  
ceramic piezoelectric materials,  
polymer piezoelectric materials,  
biomechanical energy harvesting,  
and finite element method

## Abstract

This paper investigates the influence of piezoelectric material type on the performance of biomechanical energy harvesters, with a particular focus on footstep and finger-mouse-click energy-harvesting applications. A combination of design modelling and finite element analysis was employed to assess the energy conversion efficiency of various piezoelectric materials and their adaptability to dynamic forces generated by human motion. The findings indicate that PZT5H is the most efficient material for power generation in footstep harvesters, producing the highest power output of  $3.28 \times 10^{-1} V$ . Moreover, increasing the tip mass in the footstep model was found to enhance the voltage output further, reaching up to  $3.53217 \times 10^{-1} V$ . In contrast, PZT4 exhibited the highest energy harvesting efficiency from mouse-click motion, generating a power output of  $1.17 \times 10^{-2} V$ . These findings offer in-depth insight into the capabilities of piezoelectric materials for integration into self-powered biomedical and wearable energy-harvesting applications.

## 1. Introduction

Piezoelectric energy harvesters (PEHs) function as a transducer that converts ambient mechanical energy, such as vibrations, stress, or movement, into electrical energy using the piezoelectric effect [1]. This effect occurs when piezoelectric materials generate an electric charge in response to mechanical deformation due to the orientation of their molecular structure [2]. It involves two primary mechanisms: the direct piezoelectric effect, in which mechanical stress induces an electric charge, and the reverse piezoelectric effect, in which an electric field induces mechanical deformation [3]. For vibration energy harvesting, the direct effect is particularly valuable, as it allows the conversion of ambient mechanical energy into electrical charge [4]. The generated electrical charge can be extracted for sensing and power-generation applications, making piezoelectric materials suitable for integration into a range of devices that require sustainable power sources [5].

Recent research has increasingly emphasised the utilisation of biomechanical energy derived from human activities, including walking, running, and breathing, to power low-energy devices, sensors, and wireless systems, particularly in scenarios where battery replacement is challenging or impractical [6]. Embedding PEHs into wearable devices or footwear enables the capture of energy from joint movements, foot strikes, and chest expansion during respiration [7]. This approach offers promising opportunities to power low-energy electronics such as medical implants, fitness trackers, and other wearable technologies without reliance on conventional batteries [8-10]. Additionally, investigations into energy harvesting from mouse-click motions, whether by a robotic or a human finger, demonstrate that peak energy production occurs under matched load resistance conditions [11].

However, the selection of piezoelectric material type is a critical factor that directly affects the energy-harvesting performance [12]. The crystals, such as quartz, rochelle salt, and lithium niobate, are naturally occurring but may have limited availability and performance [13]. Commonly employed material for PEHs devices, which is

Lead Zirconate Titanate (PZT) ceramics, offers high piezoelectric coefficients and permittivity but is less flexible than polymers, which may limit their suitability for conformable applications [14]. Among ceramics, Lead Zirconate Titanate 5H (PZT-5H) remains a leading candidate for biomechanical motion studies. Nevertheless, most investigations focus on high-frequency or controlled excitation environments that do not fully replicate the subtleties of human gait [15,16]. Even though Lead Zirconate Titanate 4 (PZT-4) is renowned for its durability, making it a suitable choice for a harvester, its application in biomechanical harnessing is underexplored.[17]. These materials exhibit distinct crystalline structures, piezoelectric coefficients, and mechanical properties, which critically affect their energy conversion efficiency and long-term durability [18]. Polyvinylidene fluoride (PVDF) polymers are notable for their flexibility and durability, qualities that align well with low-force, low-frequency biomechanics applications such as wearable devices [19,20]. It shows lower piezoelectric coefficients and energy-conversion efficiency than ceramics [21]. Recent work has highlighted the potential of Lead Zirconate Titanate - Lead Zinc Niobate Modified (PZT-PZNM) for energy-harvesting platforms.[22] [23]However, systematic exploration of PZT-PZNM for biomechanical energy harvesting is still in its infancy, leaving a significant gap in the literature and an opportunity for further research.

The progress of wearable technologies and self-powered biomedical devices relies heavily on the development of efficient piezoelectric energy-harvesting systems. One major challenge in this field is selecting the most appropriate materials to maximise energy conversion from biomechanical forces. Therefore, understanding the influence of piezoelectric material type on biomechanical energy-harvesting efficiency is critical for wearable and implantable technologies. The properties of materials and mechanical flexibility can vary greatly, affecting the reliability and effectiveness of the energy harvester [24]. This paper examines how the selection of piezoelectric material type influences energy output in shoe-mounted and finger-on-mouse energy harvesters. The study offers valuable insights into optimising the production of these energy harvesters under various biomechanical conditions. This was accomplished by systematically evaluating different piezoelectric materials through finite element analysis and experimental validation. These approaches enabled the optimisation of the piezoelectric energy harvester, allowing it to generate maximum energy output by capturing even subtle biomechanical motions to produce usable electrical power.

## 2. Methodology

To understand how different types of piezoelectric materials influence energy harvesting, the study systematically evaluated them through simulations and experimental validation. Customised strategies were developed to optimise the piezoelectric energy harvester (PEH) for maximum energy output, utilising biomechanical motions to generate usable electrical power. Using SolidWorks, the design models from references [11] and [6] served as a basis for creating footsteps and mouse-click models in this study. Tables 1 and 2 show the dimensions of both models.

**Table 1** Dimensions used in footsteps design<sup>[6]</sup>

Part	Length(mm)	Width(mm)	Thickness(mm)
Plate	15	15	10
Mid-plane	15	15	0.2
Piezoelectric body	47	32	0.2
Substrate	62	37	0.2
Spring	40	-	-

**Table 2** Dimensions used in mouse clicks design<sup>[11]</sup>

Part	Length(mm)	Width(mm)	Thickness(mm)
Substrate	18	8.64	0.15
Piezoelectric materials	13	8.64	0.065
Neck	5	3.00	0.215

The selected materials were applied to the corresponding body parts of both PEH models, specifically the footsteps and mouse clicks. In the T-shape design for mouse clicks, as illustrated in Fig. 1, copper was used as the bottom layer, serving as the substrate. In contrast, PZT5H, PZT4, PVDF, and PZT5A were employed as the piezoelectric top layer.

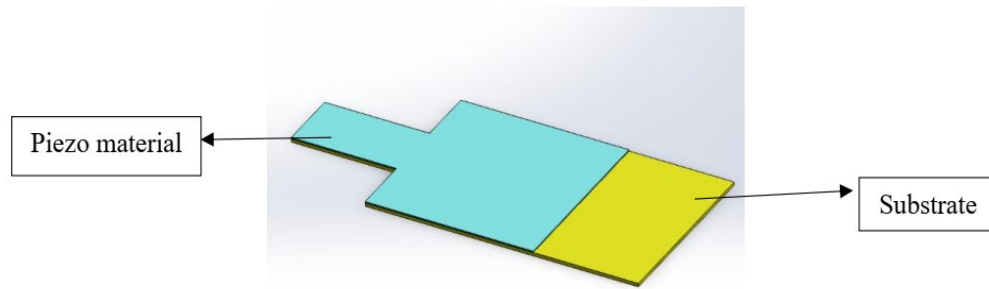


**Fig. 1** CAD design of the T-shape for mouse clicks

Fig.2 depicts the footstep design, where stainless steel was used for the plates, mini plate, substrate, and spring. At the same time, PZTPZNM, PZT5H, PVDF, and PZT4 were utilised as the piezoelectric layer.

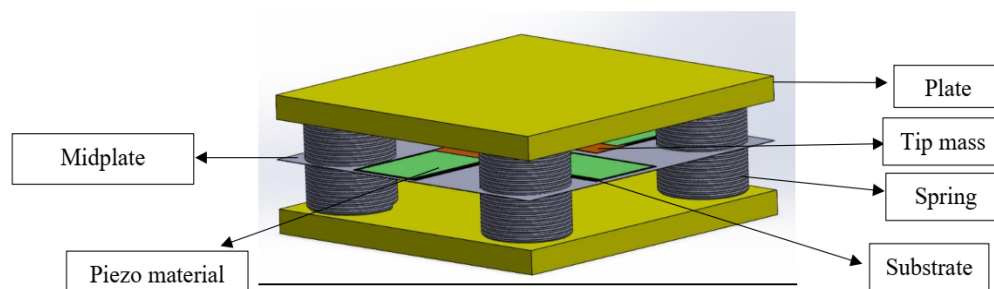


**Fig. 2** CAD design of the footstep model

After finalising the design model, it was imported into Ansys for finite element analysis. We then assigned the material properties of PZT5H, PZT4, PVDF, and PZTPZNM to the corresponding piezoelectric plates in the models. Table 3 below provides detailed material properties for the finite element analysis.

**Table 3** Materials used for each part of the PEH models

Materials	Application	Description
Copper	Used as a substrate	<ul style="list-style-type: none"> <li>Young's modulus: 120GPa</li> <li>Poisson's ratio: 0.34</li> <li>Density: 8960 kg/m<sup>3</sup></li> </ul>
Stainless Steel	Used as a substrate, spring, plates, and mini-plate	<ul style="list-style-type: none"> <li>Young's modulus: 120GPa</li> <li>Poisson's ratio: 0.34</li> <li>Density: 8960 kg/m<sup>3</sup></li> </ul>
PZT5A	Used for the piezoelectric plates	<ul style="list-style-type: none"> <li>Young's modulus: 50GPa</li> <li>Poisson's ratio: 0.35</li> <li>Density: 7750 kg/m<sup>3</sup></li> </ul>
PZT5H	Used for the piezoelectric plates	<ul style="list-style-type: none"> <li>Young's modulus: 62GPa</li> <li>Poisson's ratio: 0.31</li> <li>Density: 7500 kg/m<sup>3</sup></li> </ul>
PVDF	Used for the piezoelectric plates	<ul style="list-style-type: none"> <li>Young's modulus: 1.1GPa [40]</li> <li>Poisson's ratio: 0.34</li> <li>Density: 1780 kg/m<sup>3</sup></li> </ul>
PZTPZNM	Used for the piezoelectric plates	<ul style="list-style-type: none"> <li>Young's modulus: 120GPa</li> <li>Poisson's ratio: 0.34</li> <li>Density: 8960 kg/m<sup>3</sup></li> </ul>

The geometry was discretised to facilitate the finite element analysis of the models. The fixed support boundary conditions and forces of 825.44 N for footsteps and 0.61 N for mouse clicks were applied to simulate the model. Modal analysis was then carried out to identify natural frequencies and deformation modes. Subsequently, harmonic response analysis was performed to assess the frequency and voltage plot data for two PEH models, each using four different materials. The simulation results, including figures and tabulated data, showcase the total deformation from the modal analysis, highlighting the maximum and minimum stress range that can be achieved.

Furthermore, harmonic response analysis helps understand how models respond to varying frequencies, providing insights into their efficiency and performance under different conditions. Features such as frequency and phase response deformation are visually presented to depict the results, data, and patterns. The voltage obtained from these simulations was used to calculate output power using specific formulas, ensuring an accurate assessment of each material's energy-harvesting capabilities. The formula used to calculate the output power is as follows [10]:

$$P = (2\pi f)CV^2 \tag{1}$$

where  $P$  is the output power (in watts),  $C$  is the capacitance of the piezoelectric material (in farads),  $V$  is the voltage output of the piezoelectric material (in volts), and  $f$  is the frequency of the vibrations applied to the piezoelectric material (in hertz). Fig. 3's flowcharts outline the process of modelling and simulating the design model using finite element analysis.

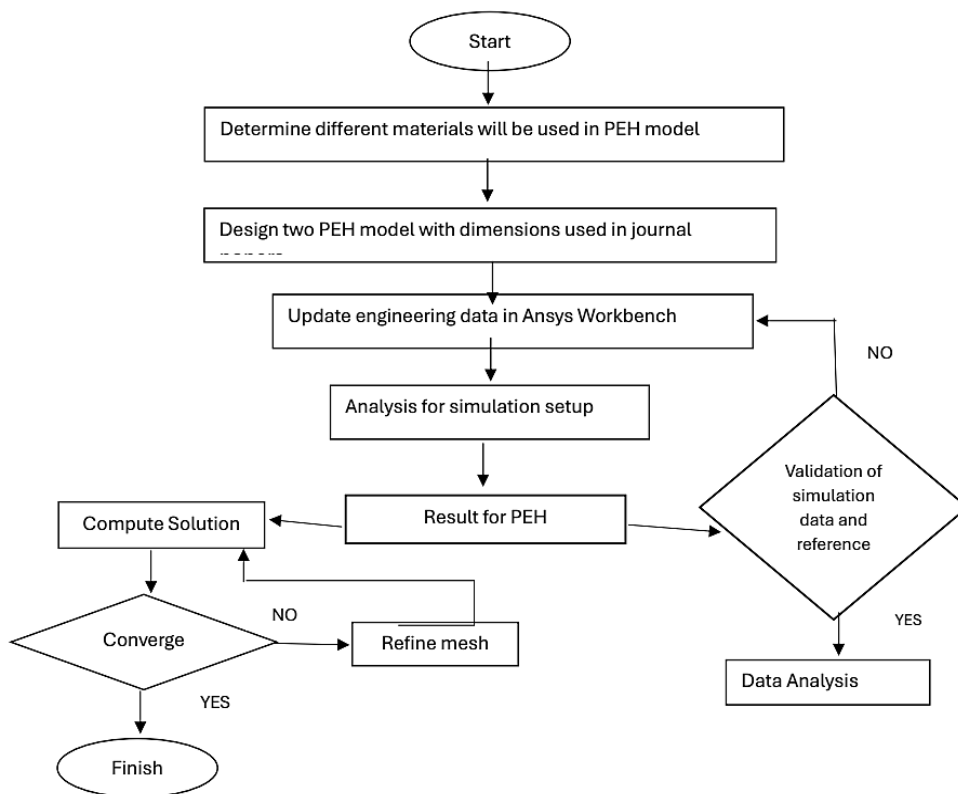


Fig. 3 Flowchart of the overview methodology

### 3. Results

The two PEH-designed models were simulated using Ansys for modal and harmonic response analyses. Initially, force data from article references is used to run the simulations and obtain results. Then, force is set to mimic actual force from human footsteps and finger mouse clicks. The highest voltage and power output values for each parameter selected throughout the simulation are tabulated.

### 3.1 Footsteps model

A comparison of simulation data for four piezoelectric materials (PZT5H, PZTPZNM, PVDF, and PZT4) under the force of footsteps, as shown in Tables 4 and 5, highlights their varying performance and efficiency.

**Table 4** Data obtained from simulating with the force of the footsteps model from the journal reference

Materials	RF(Hz)	Frequency (Hz)	Voltage(V)	Capacitance(F)	Power(W)
PZT5H	21.6	22.8	$3.11578 \times 10^{-4}$	$2.264 \times 10^{-6}$	$1.011 \times 10^{-7}$
PZTPZNM	19.2	19.2	$3.27904 \times 10^{-10}$	$1.354 \times 10^{-6}$	$2.888 \times 10^{-8}$
PVDF	20.4	21.6	$3.05078 \times 10^{-7}$	$8.0 \times 10^{-9}$	$3.020 \times 10^{-9}$
PZT4	22.8	22.8	$1.46959 \times 10^{-5}$	$0.832 \times 10^{-6}$	$1.169 \times 10^{-8}$

**Table 5** Data obtained from simulating with a force of 825.44N of the footsteps model

Materials	RF(Hz)	Frequency (Hz)	Voltage(V)	Capacitance(F)	Power(W)
PZT5H	21.6	22.8	$3.2786 \times 10^{-1}$	$2.264 \times 10^{-6}$	$3.486 \times 10^{-5}$
PZT-PZNM	19.2	19.2	$3.45003 \times 10^{-7}$	$1.354 \times 10^{-6}$	$5.286 \times 10^{-7}$
PVDF	20.4	21.6	$3.20986 \times 10^{-4}$	$8.0 \times 10^{-9}$	$3.585 \times 10^{-10}$
PZT4	22.8	22.8	$1.54623 \times 10^{-2}$	$0.832 \times 10^{-6}$	$3.015 \times 10^{-8}$

Based on Table 4, PZT5H is the most efficient material, generating the highest power output of  $3.11578 \times 10^{-4} V$  and  $1.011 \times 10^{-7} W$ , while PZT-PZNM shows the lowest performance of  $3.27904 \times 10^{-10} V$  and  $2.888 \times 10^{-8} W$ . PVDF exhibits the lowest power output of  $3.05078 \times 10^{-7} V$  and  $3.020 \times 10^{-9} W$ . PZT4 is generating a relatively high voltage of  $1.46959 \times 10^{-5} V$ . Meanwhile, in Table 5, PZT-PZNM demonstrates considerable improvement in  $3.45003 \times 10^{-7} V$  and  $5.286 \times 10^{-7} W$ . PVDF consistently exhibits the lowest power output of  $3.20986 \times 10^{-4} V$  and  $3.585 \times 10^{-10} W$ . PZT4 shows lower power output compared to PZT5H, which produced  $3.11578 \times 10^{-4} V$  and  $1.011 \times 10^{-7} W$ . Overall, PZT5H stands out as the most efficient material for energy harvesting, followed by PZT4, with PZTPZNM and PVDF exhibiting comparatively lower performance.

PZT5H is the most efficient material due to its high voltage output, substantial power, and optimal performance at a resonance frequency of 21.6 Hz, which enhances energy conversion efficiency. Its high piezoelectric coefficient allows a solid response to mechanical stress. At the same time, its balanced capacitance facilitates adequate energy storage and release. Additionally, PZT5H's consistent high efficiency across various conditions, including forces from footsteps and mouse clicks, underscores its robustness and reliability, making it the ideal choice for shoe-mounted energy-harvesting applications. PZT4 follows closely, while PZT-PZNM and PVDF exhibit comparatively lower performance. Figs. 5 and 6 show the voltage data graph for the footsteps model.

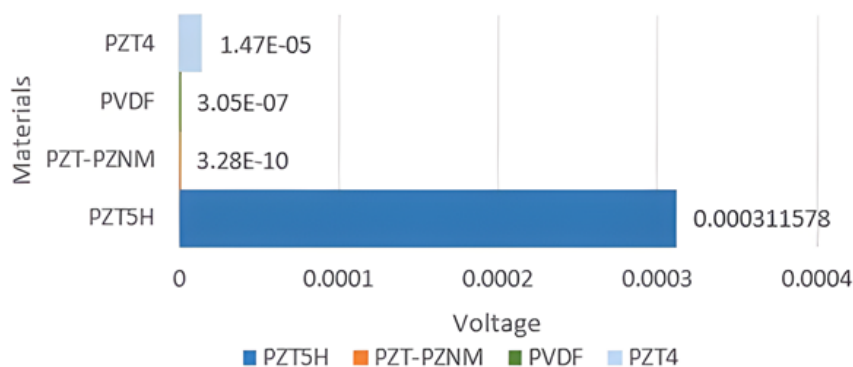


**Fig. 5** The voltage data for the Footsteps model with force are taken from the referenced article

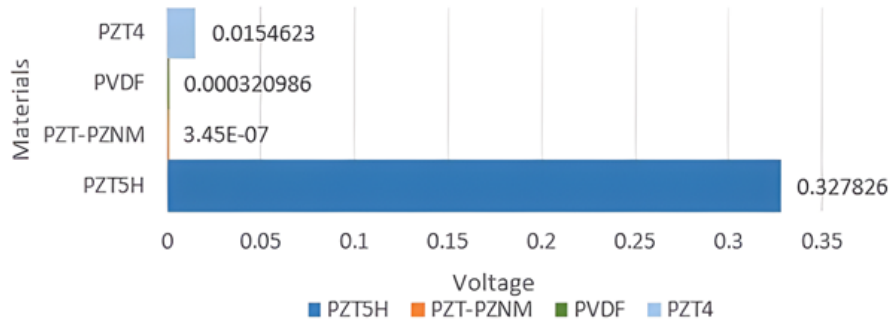


**Fig. 6** The voltage data for the footsteps model are based on the force from an average human weight of 822.5N

Table 6 presents data from simulations with various tip masses and a constant force of 825.44 N, using PZT-5H as the piezoelectric material, showing a clear trend in the generated voltage and power.

**Table 6** Data obtained from simulating with various tip masses and force 825.44N of the Footsteps model by using PZT5H as the piezoelectric material

Tip mass (g)	Frequency (Hz)	Voltage (V)	Capacitance (F)	Power (W)
0	22.8	$3.2786 \times 10^{-1}$	$2.264 \times 10^{-6}$	$3.486 \times 10^{-5}$
10	22.8	$3.32965 \times 10^{-1}$	$2.264 \times 10^{-6}$	$3.596 \times 10^{-5}$
30	22.8	$3.43091 \times 10^{-1}$	$2.264 \times 10^{-6}$	$3.818 \times 10^{-5}$
50	228	$3.53217 \times 10^{-1}$	$2.264 \times 10^{-6}$	$4.046 \times 10^{-5}$

Increasing the tip mass increases the voltage generated by PZT5H. This indicates that a heavier tip mass enhances the material's ability to convert mechanical energy into electrical energy. Specifically, the voltage rises from  $3.2786 \times 10^{-1} V$  at 0 g to  $3.5321 \times 10^{-1} V$  at 50 g. Similarly, the power output increases with increasing tip mass. Starting at  $3.486 \times 10^{-5} W$  with no added mass, it rises to  $4.046 \times 10^{-5} W$  with a 50-gramme tip mass. This indicates that the material's energy conversion efficiency improves with a heavier tip mass. The capacitance remains constant at  $2.264 \times 10^{-6} F$ , regardless of the tip mass. The frequency remains steady at 22.8 Hz throughout the simulations, ensuring that the observed changes in voltage and power are due to variations in the tip mass rather than changes in the frequency of the applied force.

In conclusion, increasing the tip mass in the footsteps model with a constant applied force of 825.44N enhances the piezoelectric performance of PZT5H. Heavier tip masses yield higher voltage and power outputs, indicating improved conversion of mechanical energy to electrical energy. This suggests that optimising the applied mass on piezoelectric materials such as PZT5H can significantly enhance their energy-harvesting capabilities in practical applications. Fig. 4 illustrates the results graphically. The analysis showed that a 50 g tip mass exerted a force of 0.4905 N on the piezoelectric material PZT5H.

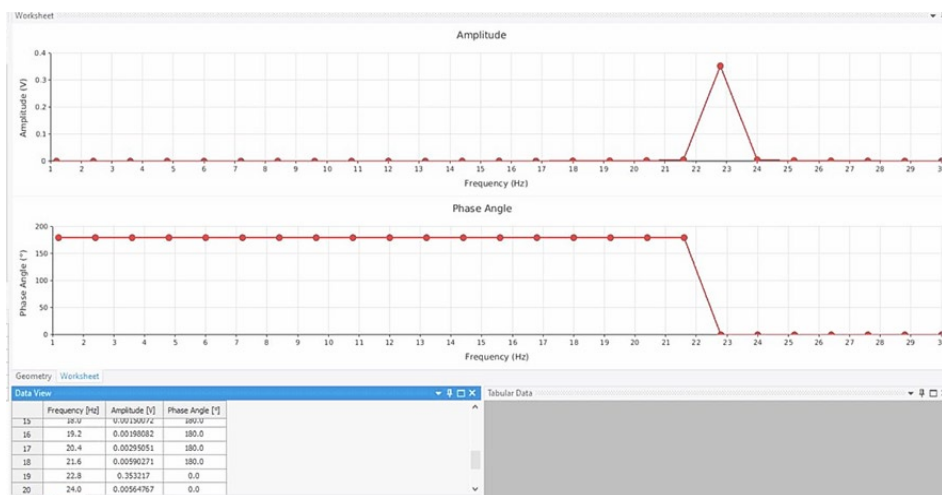


**Fig. 4** Voltage frequency plot data for the relationship of voltage amplitude for tip mass (50g) with PZT5H

According to the harmonic response plots illustrating the analysis of the piezoelectric material PZT5H, the amplitude stays low and nearly constant at most frequencies, except for a sharp peak at approximately. 22.8 Hz, where the amplitude reaches approximately.  $3.53217 \times 10^{-1} V$ , It indicates the resonance frequency. Thus, the phase angle remains constant at 180 degrees for most frequencies. Then, at the resonance frequency, it suddenly decreases to 0 degrees. This notable shift in phase angle and amplitude at 22 Hz emphasises the material's strong resonance in these conditions.

### 3.2 Mouse Clicks Model

The contrasting analysis of Tables 7 and 8 underscores PZT4 as the optimal piezoelectric material within the parameters investigated, consistently exhibiting superior voltage and power output.

**Table 7** Data obtained from simulating the force of the mouse clicks model from the journal reference

Material	RF(Hz)	Frequency (Hz)	Voltage (V)	Capacitance(F)	Power(W)
PZT5A	246.5	252	$2.12207 \times 10^{-4}$	$25.9 \times 10^{-9}$	$1.847 \times 10^{-12}$
PZT5H	247.59	252	$3.54421 \times 10^{-4}$	$52.06 \times 10^{-9}$	$1.035 \times 10^{-11}$
PZT4	264	264	$1.1668 \times 10^{-2}$	$1.869 \times 10^{-6}$	$4.221 \times 10^{-7}$
PVDF	168	168	$2.32508 \times 10^{-4}$	$19.24 \times 10^{-9}$	$1.098 \times 10^{-12}$

**Table 8** Data obtained from simulating with a force of 0.61N of the mouse clicks model

Materials	RF(Hz)	Frequency (Hz)	Voltage (V)	Capacitance(F)	Power(W)
PZT5A	246	246	$2.84626 \times 10^{-1}$	$25.9 \times 10^{-9}$	$3.243 \times 10^{-6}$
PZT5H	246	246	$2.06479 \times 10^{-1}$	$52.06 \times 10^{-9}$	$3.431 \times 10^{-6}$
PVDF	168	168	$1.38788 \times 10^{-1}$	$19.24 \times 10^{-9}$	$3.912 \times 10^{-7}$
PZT 4	264	264	6.22105	$1.869 \times 10^{-6}$	0.120

In Table 7, PZT4 generates  $1.1668 \times 10^{-2} V$  and  $4.221 \times 10^{-7} W$ , while in Table 8, it significantly increases to 6.22105 V and 0.120 W. This efficiency is attributed to its optimal resonance and operational frequency alignment at 264 Hz, high piezoelectric coefficient, and substantial capacitance of  $1.869 \times 10^{-6} F$ , It facilitates adequate energy storage and release. Overall, PZT4's superior voltage and power generation, combined with its consistently high efficiency across different conditions, make it the ideal choice for energy harvesting and sensing applications, with PZT5H also being a strong contender. PZT4 is the most efficient material due to its high voltage output, substantial power, and optimal performance at a resonance frequency of 264 Hz, which enhances energy conversion efficiency. Its high piezoelectric coefficient allows a solid response to mechanical stress, while its substantial capacitance facilitates adequate energy storage and release. Additionally, PZT4's consistent high efficiency across various conditions, such as forces from footsteps and mouse clicks, underscores its robustness and reliability, making it the ideal choice for finger-on-mouse energy harvesters. PZT5H follows closely, while PZT-5A and PVDF exhibit comparatively lower performance. The voltage data for the mouse-click model are shown in Figs. 7 and 8.

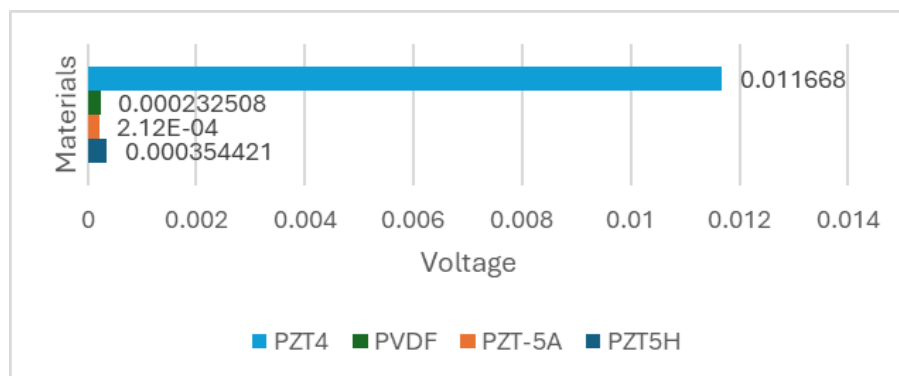


**Fig. 7** Voltage data for mouse click model from article references

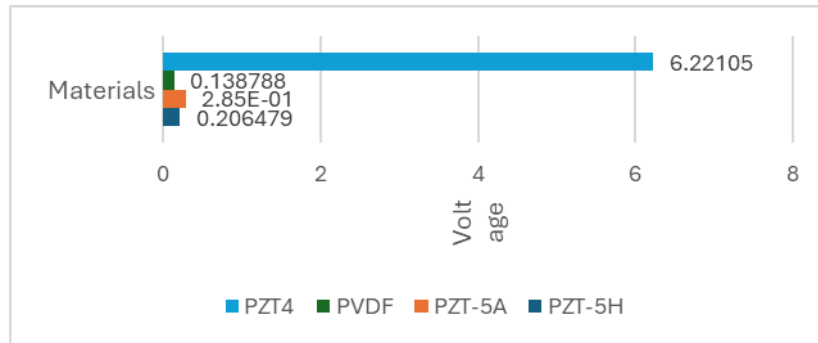


**Fig. 8** Voltage data for mouse clicks model from mouse clicks force (0.61N)

The performance difference between PZT5H and PZT4 across numerous models can be attributed to several factors, including the specific simulation settings and the materials' inherent properties. Furthermore, PZT4 has a higher piezoelectric coefficient and capacitance, making it more efficient at converting mechanical energy to electrical energy under certain conditions, particularly in simulations involving higher force magnitudes, such as mouse clicks. PZT5H, while having a slightly lower piezoelectric coefficient, still performs exceptionally well due to its optimised material properties, which are better suited to lower-frequency vibrations such as those from footsteps. The capacitance values of PZT5H and PZT4 also affect their performance; PZT4's higher capacitance enables more effective energy storage and release under higher force conditions, making it more efficient in those scenarios. PZT5H, with a balanced capacitance, performs better under conditions where the energy demands are lower and more consistent, such as the periodic force of footsteps. Variations in simulation conditions, such as the exact force applied, its duration, and the measurement metrics used (voltage vs. power output), can lead to different materials excelling in various simulations, highlighting the importance of matching the appropriate material to the specific application and operating conditions.

#### 4. Conclusion

The study successfully fulfilled its objective of investigating the influence of piezoelectric material selection on the energy output of biomechanical harvesters. The simulation results demonstrated that PZT-5H and PZT-4 exhibited superior performance compared to other materials, consistently producing the highest power output. Furthermore, increasing the tip mass in PZT-5H-based configurations further enhanced both voltage and power generation, indicating that a larger tip mass improves conversion efficiency. Similarly, PZT-4 showed excellent performance, yielding the highest voltage and power outputs, thereby establishing its suitability for finger-on-mouse energy-harvesting applications. Overall, these findings highlight the importance of selecting appropriate piezoelectric materials and optimising structural parameters to maximise energy-harvesting efficiency. The insights from this study provide a valuable reference for the design and development of next-generation biomechanical energy-harvesting devices.

#### Acknowledgement

This research was funded by a grant from the Ministry of Higher Education of Malaysia (FRGS/1/2021/TK0/USM/03/3/)

#### Conflict of Interest

The authors declare that there is no conflict of interest regarding the publication of the paper.

#### Author Contribution

The authors confirm contribution to the paper as follows: **study conception and design:** Thashayani Sathasivam, Nur Hidayah Mansor; **analysis and interpretation of results:** Thashayani Sathasivam; **draft manuscript preparation:** Thashayani Sathasivam, Nur Hidayah Mansor. All authors reviewed the results and approved the final version of the manuscript.

#### References

- [1] Zhou, W., Du, D., Cui, Q., Lu, C., Wang, Y., & He, Q. (2022). Recent Research Progress in Piezoelectric Vibration Energy Harvesting Technology. *Energies*, 15(3), 947. <https://doi.org/10.3390/en15030947>

- [2] Covaci, C., & Gontean, A. (2020). Piezoelectric Energy Harvesting Solutions: A Review. *Sensors*, 20(12), 3512. <https://doi.org/10.3390/s20123512>
- [3] Moghadasi, K., Mohd Isa, M. S., Ariffin, M. A., Mohd jamil, M. Z., Raja, S., Wu, B., Yamani, M., Bin Muhamad, M. R., Yusof, F., Jamaludin, M. F., Ab Karim, M. S. bin, Abdul Razak, B. binti, & Yusoff, N. bin. (2022). A review on biomedical implant materials and the effect of friction stir based techniques on their mechanical and tribological properties. *Journal of Materials Research and Technology*, 17, 1054-1121. <https://doi.org/10.1016/j.jmrt.2022.01.050>
- [4] Yang, Z., Zhou, S., Zu, J., & Inman, D. (2018). High-Performance Piezoelectric Energy Harvesters and Their Applications. *Joule*, 2(4), 642-697. <https://doi.org/10.1016/j.joule.2018.03.011>
- [5] Kapadi, N. J., Jadhav, T. K., Darvade, T. C., Mahesh, M. L. V., & Kambale, R. C. (2025). Morphotropic phase boundary driven Na 0.5 Bi 0.5 TiO 3 –BaTiO 3 based lead-free ceramics with dual functionality in energy harvesting and piezo stack actuation. *Journal of Alloys and Compounds*, 1041. <https://doi.org/10.1016/j.jallcom.2025.183730>
- [6] Zhao, B., Qian, F., Hatfield, A., Zuo, L., & Xu, T.-B. (2023). A Review of Piezoelectric Footwear Energy Harvesters: Principles, Methods, and Applications. *Sensors*, 23(13), 5841. <https://doi.org/10.3390/s23135841>
- [7] Li, Q., Naing, V., & Donelan, J. M. (2009). Development of a biomechanical energy harvester. *Journal of NeuroEngineering and Rehabilitation*, 6(1), 22. <https://doi.org/10.1186/1743-0003-6-22>
- [8] Sharma, S., Kiran, R., Azad, P., & Vaish, R. (2022). A review of piezoelectric energy harvesting tiles: Available designs and future perspective. *Energy Conversion and Management*, 254, 115272. <https://doi.org/10.1016/j.enconman.2022.115272>
- [9] Serrano, M., Larkin, K., Tretiak, S., & Abdelkefi, A. (2023). Piezoelectric Energy Harvesting Gyroscopes: Comparative Modeling and Effectiveness. *Energies*, 16(4), 2000. <https://doi.org/10.3390/en16042000>
- [10] Dewanjee, J., & Islam, M. S. (2024). Piezoelectric based V-shape cantilever beam design of energy harvester for biomedical applications. *International Review of Applied Sciences and Engineering*, 15(1), 73-81. <https://doi.org/10.1556/1848.2023.00652>
- [11] Uddin, Md. N., Islam, Md. S., Sampe, J., Bhuyan, M. S., & Ali, S. H. Md. (2016). Design and Analysis of a T-shaped Piezoelectric Cantilever Beam at Low Resonant Frequency using Vibration for Biomedical Device. *Asian Journal of Scientific Research*, 9(4), 160-166. <https://doi.org/10.3923/ajsr.2016.160.166>
- [12] Sun, Y., Tan, T., & Yan, Z. (2025). Smart Ocean powering and sensing via mechanical energy harvesting: Methods, advances, and challenges. *Nano Energy*, 141. <https://doi.org/10.1016/j.nanoen.2025.111128>
- [13] Vatanpour, V., Rezaia, H., Al-Shaeli, M., & Khataee, A. (2025). Advances in self-cleaning membranes for effective water and wastewater treatment. *Separation and Purification Technology*, 373. <https://doi.org/10.1016/j.seppur.2025.133539>
- [14] Wei, J., Hu, X., Li, Y., Bian, Z., Yan, K., & Wu, D. (2025). 3D-printed piezoelectric ceramics with auxetic structure for high-performance sensing applications. *Ceramics International*, 51. <https://doi.org/10.1016/j.ceramint.2024.11.234>
- [15] Brusa, E., Carrera, A., & Delprete, C. (2023). A Review of Piezoelectric Energy Harvesting: Materials, Design, and Readout Circuits. *Actuators*, 12(12), 457. <https://doi.org/10.3390/act12120457>
- [16] Abhijith, V., Akhila, B., Pramod, K., Mohanty, T. R., Sivakumar, C., Ramakrishnan, S., Thomas, S., & Sreekala, M. S. (2025). Recent advances in metal oxide reinforced polymer composites for efficient piezoelectric energy harvesting applications. *Applied Energy*, 397. <https://doi.org/10.1016/j.apenergy.2025.126335>
- [17] Dastgir, N., Ansari, R., Hassanzadeh-Aghdam, M. K., & Sahmani, S. (2025). Finite element analysis of the electro-mechanical behaviors of piezocomposite bimorph energy harvesters under static and dynamic loadings. *Composites Communications*, 59. <https://doi.org/10.1016/j.coco.2025.102573>
- [18] Mahapatra, S. Das, Mohapatra, P. C., Aria, A. I., Christie, G., Mishra, Y. K., Hofmann, S., & Thakur, V. K. (2021). Piezoelectric Materials for Energy Harvesting and Sensing Applications: Roadmap for Future Smart Materials. *Advanced Science*, 8(17). <https://doi.org/10.1002/advs.202100864>
- [19] Emara, A. I., Shahba, A. F., Ali, G., Mamdouh, M., Abdellatif, S. O., Nassar, K., & Hamouda, T. (2025). Enhanced energy harvesting from NF-PVDF piezoelectric material for wearable electronics: I- V characterisation and charge-discharge performance. *Materials for Renewable and Sustainable Energy*, 14(2), 45. <https://doi.org/10.1007/s40243-025-00321-x>
- [20] Ebrahimi, F., & Ahari, M. F. (2024). Mechanics of Active Materials. İçinde *Comprehensive Mechanics of Materials*. <https://doi.org/10.1016/B978-0-323-90646-3.00043-5>

- [21] Nivedhitha, D. M., Jeyanthi, S., Rithish, B., Charan, B. G. S., Ravi, S., Vinayagamurthy, G., & Thiagamani, S. M. K. (2025). An experimental analysis of air flow-induced piezoelectric energy harvesting using flexible poly (vinylidene fluoride) nanocomposite films. *Discover Materials*, 5(1), 12. <https://doi.org/10.1007/s43939-025-00190-1>
- [22] Bakhtiar, S. U. H., Hussain, S. abbas, Ali, S., Ismail, A., Zada, A., Sattar, H., Raziq, F., Zahid, M., Al-Fatesh, A. S., Dong, W., & Fu, Q. (2024). Innovative perspectives on porous ferroelectric ceramics and their composites: Charting new frontiers in energy applications. *Materials Today Communications*, 38. <https://doi.org/10.1016/j.mtcomm.2024.108388>
- [23] Wang, X., Wang, Y., Zhang, Y., Wang, H., Gu, Z., & Zou, H. (2022). Enhancement of the piezoelectric property in PMN-PZT/PZT thin films. *Ceramics International*, 48(9), 12813-12818. <https://doi.org/10.1016/j.ceramint.2022.01.152>
- [24] Krishnaveni, C., Muthuramalingam, M., Sateesh, D., Manojkumar, K., Boominathan, J., Hajra, S., Panda, S., Kim, H. J., Sundaramoorthy, A., & Vivekananthan, V. (2025). Interfacial Engineering in Wearable Piezoelectric Nanogenerators: A Path to Sustainable Future in Self-Powered Electronics. *Advanced Sustainable Systems*, 9. <https://doi.org/10.1002/adsu.202400884>